Organic & Biomolecular Chemistry

Accepted Manuscript

ROYAL SOCIETY OF CHEMISTRY

www.rsc.org/obc

Theoretical study of the reaction of hydroxyl radical with uridine: the influence of ribose and solvent

Ya Gao, Xiayu Chen, Li Zhong, Wei Yao, Shujin Li*

College of Chemistry, Chemical Engineering and Materials Science, Soochow University PR China，215123

The reaction of hydroxyl radical (•OH) with uridine has been investigated using density functional theory (DFT). The influence of environment has been investigated using water and benzene as models for polar and non-polar surroundings, in addition to gas phase calculations. In order to represent a much more real situation in the RNA, the ribose of the uracil ring is considered. Different paths of the reaction of •OH with uridine have been considered, involving addition and hydrogen abstraction reactions, with global contributions to the overall reaction around 99.9% and 0.1% at 298K, respectively. The *cis*- and *trans*- U5OH addition reactions contribute to the overall reaction around 62.2% and 35.6% in the polar surrounding and about 70.1% and 26.8% in the non-polar surrounding, respectively. The *cis*-U5OH adduct is found to be the major product of the title reaction for all the modeled environments. The steric effect of the ribose of the uracil ring makes the U6OH addition more difficult than the U5OH addition. The theoretical study of the reaction of •OH with uridine could help us to understand the oxidative damage of DNA and RNA better. The good agreement found between the calculated and the available experimental data supports the methodology used in this work, as well as the data reported here for the first time.

[a] To whom correspondence should be addressed. E-mail: shujinli@suda.edu.cn.

Introduction

As is known, DNA and RNA oxidative damage can cause several diseases like cancer, cardiovascular disorders, and atherosclerosis.[1,2] Reactive oxygen species (ROS), is considered as one of the main factor causing DNA and RNA oxidative damage. The ROS, such as superoxide radical anion (O_2^-), perhydroxyl radical (HO_2•), and hydroxyl radical (•OH), are normal organism metabolites which are formed in vast quantities in each cell every day. The •OH radical is the most reactive ROS,[3] and due to its high reactivity the hydroxyl radical (•OH) is chosen for this study.

In previous investigations, the nucleic acid bases are often used as models to examine the properties of nucleotides or nucleosides. The reaction of nucleic acid bases with •OH radical has been studied experimentally and theoretically. The •OH is electron-deficient radical, thus mainly the •OH reacts with the nucleic acids through addition modes on the base units or by abstracting hydrogen atoms from the base. Pulse radiolysis and laser photolysis experiments have been done to obtain the information about the transients produced from the reactions of •OH with nucleic acid bases.[4] It shows that •OH has high reactivity towards nucleic acid with almost diffusion controlled rates (10^9–10^{10} dm^{-3} mol^{-1} s^{-1}). Pulse radiolysis experiments on some pyrimidines analysis using HPLC with UV detection coupled to a mass spectrometer through an electrospray interface (HPLC-ES-MS) clearly demonstrated that •OH generally undergoes addition reaction at C5C6 double bond,[5] and previous experimental studies showed that the •OH addition to the C5C6 double bond of pyrimidine nucleobases is more regioselective to the C5 atom than the C6 atom.[6-11]

As the simplest pyrimidine base of RNA, the reaction of •OH with uracil has been studied theoretically. The relative energies for the some stationary points along the addition reaction path and hydrogen abstraction reaction path were calculated at the MPW1K/6-31+G(d,p), CCSD(T)//B3LYP/6-31+G(d,p), and CCSD(T)//MPW1K/6-31+G(d,p) levels.[12] The theoretical results showed that the possibility of reaction followed the order •OH-addition at C6 > •OH-addition at C5 > H8-abstraction from N3.

However, to our best knowledge, the reaction of •OH with uridine has not been studied. The influence of the sugar-ring of the uracil on the title reaction has not been known. The proton transfer process of uridine has been studied theoretically, it suggested that the introduction of sugar-ring changed the activation energy during the monohydrated proton transfer of uridine.[13] As an important constituent of the nucleotides, the ribose will certainly have some influence on the title reaction. In order to represent a more authentic situation, it is necessary to take the sugar-ring into consideration. Therefore, the objective of this work is to provide quantitative information about mechanism and kinetics of the reaction of •OH with uridine in gas phase, polar and non-polar surroundings, which can be considered as the very first step in the oxidative damage of RNA. It is also our purpose to obtain branching ratios for the different channels. The research on mechanism of DNA and RNA oxidative damage caused by ROS has fatal significance in disease diagnosis, drug development, and environmental assessment of chemical reagents, so a detailed understanding of the mechanism is highly urgent.

Computational details

Electronic structure calculations have been performed with the Gaussian 03 program.[14] Full geometry optimizations and frequency calculations were carried out for all the stationary points

using the density functional theory method B3LYP[15-17] with the basis set 6-311+G(d,p)[18]. Local minima and transition states were identified by the number of imaginary frequencies (NIMAG=0 or 1, respectively). In addition, transition states were verified to connect the designated reactants with products by performing an intrinsic reaction coordinate (IRC) analysis.[19] Solution phase optimizations were performed at B3LYP/6-311+G(d,p) level using the polarizable continuum model (PCM),[20] specifically theintegral-equation-formalism (IEF-PCM),[21] with water and benzene as solvents for polar and non-polar environments, respectively.

The rate constants were calculated using the POLYRATE 9.7 program.[22] The small-curvature tunneling (SCT) correction method was used in our calculation of the rate constants. In order to calculate the rate constants, 10 points near the transition state along the minimum energy path were selected - 5 points on the reactant side and 5 points on the product side. For each point, the frequency is calculated to obtain the information of Cartesian coordinates, gradient and Hessian matrix.

Results and discussion

The different reactive sites that have been studied in the present work are schematically represented in Fig. 1. The reaction of •OH with uridine undergoes mainly addition and hydrogen abstraction reactions. The •OH adds to C5 and C6 atoms of uracil ring is denoted as U5OH and U6OH path, respectively. The •OH attack to the uracil ring can show *cis*- or *trans*- addition path with respect to the ribose if we take the uracil ring as a reference plane. The •OH also abstracts hydrogen atom from N3, C5 and C6 atoms, denoted as UN3H8, UC5H10, UC6H11 path, respectively.

The optimized geometry of uridine is depicted in Fig. 2 with selected bond lengths. The distance of C5C6 bond is 1.350 Å and is substantially shorter than the rest, which indicates a localized double bond character for this bond. The highest occupied orbital (HOMO) is located on the C5C6 double bond, which brings out that C5 and C6 are electron rich centers. Hence, the electrophilic additions of •OH would have a high preference on the two atoms.

The optimized geometries of the transition states (TS) with imaginary frequencies and adducts in gas phase are shown in Fig. 3. The reaction barriers ($\Delta G^{\neq}$) and reaction Gibbs free energies (ΔG) at 298 K for the different reaction paths of the •OH with uridine reaction in the gas, water and benzene phases are listed in Table 1. The optimized geometry parameters of all the stationary points in the gas, water and benzene phases are reported in Table S1 (as supplementary information). The optimized geometries for complexes of uridine with one water molecule in the aqueous media along with ΔG (in kcal mol^{-1}) and transition states of *cis*-U5*wa*OH and *trans*-U5*wa*OH paths in the presence of one water molecule in the aqueous media along with imaginary frequencies are shown in Fig.S1(as supplementary information).

As shown in Fig. 3, the O···C5(6) distances of transition states (*cis*-C5OH-TS, *trans*-C5OH-TS, *cis*-C6OH-TS and *trans*-C6OH-TS) in the U5OH and U6OH addition paths are very similar, around 2.1 Å, suggesting that all the addition paths should have similar heats of reaction. For hydrogen abstraction paths, the N···H or C···H distances of transition states (UN3H8-TS, UC5H10-TS and UC6H11-TS) increase by 15.3%-21.1% compared to uridine, and the O···H distance increased by 17.1%-20.6% compared to water.

As the values in Table 1 show, all the paths except UC5H10 are predicted to be exergonic, the

reaction Gibbs free energies (ΔG_{gas}) are in the range of -12.74 to 0.75 kcal mol^{-1}. In addition, the energy releases associated with the adduct formation are larger than those of the hydrogen abstraction paths. The larger exergonicities were found for the U5OH adduct and U6OH adduct, especially the *cis*-U6OH adduct, ΔG_{gas} = -12.74 kcal mol^{-1}, suggesting that *cis*-U6OH adduct is the most stable addition product thermodynamically. This is due to the formation of the hydrogen bond O9'-H···O12 between the sugar-ring and the base (uracil ring) as shown in Fig. 3. The hydrogen bond distance and angle are 1.962Å and 168.6°, respectively. The reaction barriers ($\Delta G_{gas}^{\neq}$) range from 1.87 to 12.48 kcal mol^{-1}. The barriers of U5OH paths are lower than those of U6OH paths in all the modeled surroundings as shown in Table 1, indicating that U5OH is the favorable addition path. The barrier of the *cis*-U5OH path is lower than that of the *trans*-U5OH path by 2.11 kcal mol^{-1}, suggesting that U5OH adducts should be mainly formed as *cis*-U5OH. This is caused by the formation of the hydrogen bond O9'-H···O12 in the *cis*-U5OH path. For the U6OH path, on the other hand, the barrier of *cis*-U6OH path almost equals to that of *trans*-U6OH path. Therefore, we can conclude that the *cis*-U6OH and *trans*-U6OH adducts are expected to occur in similar proportions.

The previous calculation showed that the reaction trend for •OH + uracil was •OH-addition at C6 atom> •OH-addition at C5 atom.[12] Experiments showed that the •OH addition to pyrimidine nucleobases is more regioselective to the C5 atom than the C6 atom. [6-11] In this study, the reaction of •OH with uracil has also been calculated at the same level of theory to investigate the influence of the steric effect of the sugar-ring. As shown in Table 1, the barriers of U5OH and U6OH paths in the •OH + uracil reaction are 4.55 and 4.63 kcal mol^{-1}, respectively. The energy barrier of the •OH addition to both C5 and C6 positions of uracil is less than 1 kcal mol^{-1}. This indicates •OH addition to uracil is a little more regioselective to the C5 atom than the C6 atom. If we take the sugar-ring into consideration, the situation has changed. For the •OH + uridine reaction, the barrier difference between U5OH path and U6OH path is apparent as shown in Table 1. The barriers of *cis*-U5OH path and *trans*-U5OH path are 1.87 and 3.98 kcal mol^{-1} lower than those of *cis*-U6OH and *trans*-U6OH, respectively. Therefore, due to the steric effect of the ribose, the •OH addition to urdine is more regioselective to the C5 atom than the C6 atom. The *cis*-U5OH path is more regioselective than the *trans*-U5OH path. This is because the hydrogen bond O9'-H···O12 between the sugar-ring and the base (uracil ring) exists in the *cis*-U5OH-TS. Consistent with the barriers of the •OH + uridine reaction, relative possibilities of addition reaction follow the order, *cis*-U5OH＞*trans*-U5OH＞*trans*-U6OH＞*cis*-U6OH in gas phase, which is in line with the HOMO of uridine shown in Fig. 2. The *cis*-U5OH path is the most favorable path among the four addition paths.

The barriers of the hydrogen abstraction paths (UC6H11, UN3H8, and UC5H10) are in the range of 9.11 to 12.48 kcal mol^{-1}, which are higher than those of C5C6 double bond addition paths. As shown in Table 1, the relative possibilities of hydrogen abstraction reaction follow the order, UN3H8＞UC5H10＞UC6H11. We also investigate the hydrogen abstraction paths of •OH with uracil at B3LYP/6-311+G(d,p), the barriers of the hydrogen abstraction paths (UC6H11, UN3H8, and UC5H10) are in the range of 9.51 to 11.34 kcal mol^{-1}, the relative possibilities of hydrogen abstraction reaction follow the order, UC6H11＞UN3H8＞UC5H10. Due to the steric effect of the ribose, the •OH abstraction hydrogen from C6 atom of uridine is more difficult. In conclusion, the ribose does have some influences on the nucleic bases during the reaction, and it is very necessary to take the sugar-ring into consideration.

The effect of solvent is also taken into account using water and benzene as models for polar and non-polar surroundings. The solvent have little effect on the structures as shown in Table S1. To investigate the effect of hydrogen bond between water and uridine on the reaction in the aqueous media, we calculate all the optimized geometries of uridine through hydrogen bonding with one water molecule, and obtained four uridine + H_2O complexes: U-H_2O*a*, U-H_2O*b*, U-H_2O*c* and U-H_2O*d*. The optimized geometries and Gibbs free energies (ΔG) of the complexes are shown as in Fig. S1. The most stable complex is U-H_2O*a* in which H_2O makes two simultaneous hydrogen bonds with the H8 and O9 atom of uridine. The result is consistent with the previous study.[23,24] We also investigate the two reaction paths which •OH adds to the C5 atom of the U-H_2O*a* complex in the aqueous media (denoted as *cis*-U5*wa*OH and *trans*-U5*wa*OH paths). The reaction barriers ($\Delta G_{water}^{\neq}$ and $\Delta G_{benzene}^{\neq}$) and the reaction Gibbs free energies (ΔG_{water} and $\Delta G_{benzene}$) at 298 K with water and benzene as solvent are listed in Table 1. Comparing the values with those in gas phase, the reaction barriers of all the reaction paths are found to be systematically higher in the water phase than those in gas phase by 1.05-2.45 kcal mol^{-1}. The reaction barriers ($\Delta G^{\neq}$) of *cis*-U5*wa*OH and *trans*-U5*wa*OH paths are 3.69 and 4.10 kcal mol^{-1}, respectively, and are still higher than those in gas phase as shown in Table 1. The hydrogen bond between uridine and one water molecule has a very small influence on the addition reaction barriers in the aqueous media. However, the reaction barriers were found to be systematically lower in the benzene phase than in gas phase by 0.37-1.33 kcal mol^{-1}.The reaction is the easiest in non-polar surrounding, and is the hardest in polar surrounding. Although the reaction barriers ($\Delta G^{\neq}$) are different, relative possibilities of the reactions follows the order, *cis*-U5OH > *trans*-U5OH > *trans*-U6OH > *cis*-U6OH > UN3H8 > UC5H10 > UC6H11, for all the modeled environments. Therefore, the relative probabilities for the addition and hydrogen abstraction reactions that •OH can induce in uridine are similar in gas, water and benzene phase. We suggest that •OH with nucleic acid bases reaction can be modeled in vacuum phase, which is in agreement with the suggestions by Ji et al.[25,26] The Gibbs free energies of *cis*-U6OH and *trans*-U6OH are -8.28 and -8.49 kcal mol^{-1} in the water, they are -10.27 and -10.87 kcal mol^{-1} in the benzene, respectively. The solvent effect makes the *cis*-U6OH adduct and *trans*-U6OH adduct the same stable addition product thermodynamically.

The canonical variational transition state theory (CVT) with small-curvature tunneling (SCT) effect is effective to calculate the rate constants, which have been successfully applied to many reactions.[27-29] Because uridine is RNA's characteristics base and usually people's body temperature always remains at a constant 310K, then the overall rate constants at 298 K and 310 K are calculated. The branching ratios are calculated as:

$$\Gamma_{path} = \frac{k_{path}}{k_{overall}}$$

in such way that the rate constant for each path can be obtained by multiplying the overall rate constant by the corresponding Γ value. The CVT rate constants with the SCT correction and branching ratios are shown in Table 2.

The rate constant in aqueous solution at 298 K has been previously reported by different authors , 5.7×10^9 dm^{-3} mol^{-1} s^{-1} and 3.1×10^9 dm^{-3} mol^{-1} s^{-1} for the •OH + uracil reaction,[4,30] and 5.2×10^9 dm^{-3} mol^{-1} s^{-1} for the •OH + uridine reaction.[4] The calculated rate constant in this work is 2.74×10^9 dm^{-3} mol^{-1} s^{-1} in the water phase at 298 K which is in good agreement with the

experimental result.[4]

Analyzing the results reported in Table 2, it can be easily seen that regardless of the polarity of the environment, the U5OH paths occur easily since the rate constants are very large owing to the low barriers. The C5C6 double bond in uridine is preferentially attacked at the electron-richer C5 by •OH as discussed above. As the polarity of the environment increases, so does the extent to which the U5OH adducts are formed: 94.4%, 96.1% and 97.3% in gas phase, benzene and water phase at 310K. The main product is the *cis*-U5OH adduct in all the modeled media. The branching ratio of *cis*-U5OH is 66.5%, 65.3% and 59.0% in gas, benzene and water phase at 310K, respectively. On the other hand the extent to which U6OH adducts are formed decreases from gas phase (5.5%) to benzene (3.7%) to water phase (1.7%). The *cis*- U6OH and *trans*-U6OH adducts are occur in similar proportions. The kinetic factors are more dominant than the thermodynamic factors in the reaction of •OH with uridine, which is in agreement with previous studies.[25,26,31,32] The hydrogen abstraction products (such as UN3H8, UC5H10 and UC6H11) can be neglected since the corresponding paths of reaction contribute to the overall rate constant by less than 0.2% in all the cases. Previous experimental data showed that 82% and 18% of the reaction products correspond to U5OH and U6OH adducts in the •OH + uracil reaction in aqueous solution at 298K, respectively.[4] Due to the the steric effect of the sugar-ring, the branching ratios of U5OH adduct and U6OH adduct in the •OH + uridine reaction in aqueous solution are 98% and 2% in this study, respectively.

Conclusions

The present theoretical study has provided valuable information about the energetics of the reaction mechanism of •OH with uridine. Different paths of reaction have been considered, involving •OH additions to and H abstractions from uridine. Obviously, the •OH addition reactions are preferable than the hydrogen abstraction reactions. Thermodynamically, the *cis*-U6OH adduct is the most stable product. However, the addition of •OH to C5 is predicted to be the main path. This indicates that the kinetic factors are more dominant than the thermodynamic factors. The sugar-ring and solvent effect are considered. The introduction of the sugar-ring has strongly influenced the relative site reactivity. It makes the •OH addition to uridine is more regioselective to the C5 atom than the C6 atom. The U5OH path reaction is easiest in non-polar surrounding, and is hardest in polar surrounding. The hydrogen bonding between one water molecule and uridine has a very small influence on the addition reaction barriers in the aqueous media. In addition, the relative probabilities for the reactions follow the same order for all the modeled environments. The direct dynamic calculation is performed and the rate constants are calculated. The calculated and the available experimental rate constant for this reaction is around 10^9 dm^{-3} mol^{-1} s^{-1} in aqueous solution at 298 K, the good agreement between them supports the methodology used in this work.

This paper is the first attempt to study the reaction of •OH with uridine. Consideration of the ribose's influence and solvent effect provides more interesting results. The model of nucleic acid bases with the sugar fragment represents a much more real situation in the helical structures of RNA.

Acknowledgements

The authors thank the Nation Science Foundation of China (No.20977064) for the financial support to this work and also thank the project funded by the priority academic program development of Jiangsu higher education institutions.

References

1 G. S. Omenn, G. E. Goodman and M. D. Thornquist, *N. Engl. J. Med*., 1996, **334**, 1150.
2 L. H. Kushi, A. R. Folsom and R. J. Prineas, *N. Engl. J. Med*., 1996, **334**, 1156.
3 D. L. Zhang, S. J. Zhu and G. F. Luo, *J of China three gorges univ*., 2004, **26**, 563.
4 C. von Sonntag, *Free-radical-induced DNA damage and its repair: a chemical perspective,* Springer, 2006, ch.10, pp. 234-238.
5 T. L. Luke, T. A. Jacob and H. Mohan, *J. Phys. Chem. A*., 2002, **106**, 2497.
6 E. Hayon and M. Simic, *J. Am. Chem. Soc*., 1973, **95**, 1029.
7 S. Fujita and S. Steenken, *J. Am. Chem. Soc*., 1981, **103**, 2540.
8 M. Al-Sheikhly and C. Von Sonntag, *Z. Naturforsch*., 1983, **38**, 1622.
9 S. V. Jovanovic and M. G. Simic, *J. Am. Chem. Soc*., 1986, **108**, 5968.
10 S. Steenken, *Chem. Rev*., 1989, **89**, 503.
11 D. K. Hazra and S. Steenken, *J. Am. Chem. Soc*., 1983, **105**, 4380.
12 K. P. Prasanthkumar, C. H. Suresh and C. T. Aravindakumar, *Radiat. Phys. Chem*., 2012, **81**, 267.
13 L. Zhang, H. Li and X. Hu, *Chem. Phys*., 2007, **337**, 110.
14 M. J. Frisch, G. W. Trucks, H. B. Schlegel, G. E. Scuseria, M. A. Robb, J. R .Cheeseman, J. A. Montgomery, Jr., T. Vreven, K. N. Kudin, J. C. Burant, J. M. Millam, S. S. Iyengar, J. Tomasi, V. Barone, B. Mennucci, M. Cossi, G. Scalmani, N. Rega, G. A. Petersson, H. Nakatsuji, M. Hada, M. Ehara, K. Toyota, R. Fukuda, J. Hasegawa, M. Ishida, T. Nakajima, Y. Honda, O. Kitao, H. Nakai, M. Klene, X. Li, J. E. Knox, H. P. Hratchian, J. B. Cross, V. Bakken, C. Adamo, J. Jaramillo, R. Gomperts, R. E. Stratmann, O. Yazyev, A. J. Austin, R. Cammi, C. Pomelli, J. O chterski, P. Y. Ayala, K. Morokuma, G. A. Voth, P. Salvador, J. J. Dannenberg, V. G. Zakrzewski, S. Dapprich, A. D. Daniels, M. C. Strain, O. Farkas, D. K. Malick, A. D. Rabuck, K. Raghavachari, J. B. Foresman, J. V. Ortiz, Q. Cui, A. G. Baboul, S. Clifford, J. Cioslowski, B. B. Stefanov, G. Liu, A. Liashenko, P. Piskorz, I. Komaromi, R. L .Martin, D. J. Fox, T. Keith, M. A. Al-Laham, C. Y. Peng, A. Nanayakkara, M. Challacombe, P. M. W. Gill, B. G. Johnson, W. Chen, M. W. Wong, C. GonzalezandJ. A. Pople, GAUSSIAN 03 (RevisionD.01), Gaussian, Inc., Wallingford, CT, 2004.
15 A. D. Becke, *J. Chem. Phys*., 1993, **98**, 5648.
16 C. T. Lee, W. T. Yang and R. G. Parr, *Phys. Rev*., 1988, **37**, 785.
17 B. Miehlich, A. Savin and H. Stoll, *Chem. Phys. Lett*., 1989, **157**, 200.
18 M. J. Frisch, J. A. Pople and J. S. Binkley, *J. Chem. Phys*., 1984, **80**, 3265.
19 C. Gonzales and H. B. Schlegel, *Chem. Phys*., 1989, **90**, 2154.
20 B. Mennucci and J. Tomasi, *J. Chem. Phys*., 1997, **106**, 5151.
21 (a) M. T. Cances, B. Mennucci and J. Tomasi, *J. Chem. Phys*., 1997, **107**, 3032; (b) B. Mennucci and J. Tomasi, *J. Chem. Phys*., 1997, **106**, 5151; (c) B. Mennucci, E. Cances and J. Tomasi, *J. Phys. Chem. B.*, 1997, **101**, 10506; (d) J. Tomasi, B. Mennucci and E. Cances, *THEOCHEM*, 1999, **464**, 211.

22 J. C. Corchado, Y. Y. Chuang and P. L. Fast, POLYRATE, version 9.7, University of Minnesota, Minneapolis, 2007.
23 M. P. Gaigeot, N. Leulliot and M. Ghomi, *Chem. Phys*., 2000, **261**, 217.
24 M. P. Gaigeot, C. Kadri and M. Ghomi, *J. Mol. Struct.,* 2001, **565**, 469.
25 Y. Ji, Y. Xia and M. Zhao, *Int. J. Quantum Chem.,* 2005, **101**, 211.
26 Y. Ji, Y. Xia and M. Zhao, *J. Mol. Struct.: THEOCHEM*, 2005, **723**, 123.
27 T. Sun, Q. Zhang and X. Qu, *Chem. Phys. Lett*., 2005, **407**, 527.
28 Q. Zhang, R. O. Zhang and Y. Gu, *J. Phys. Chem. A.*, 2004, **108**, 1064 .
29 T. Sun, Y. Wang and C. Zhang, *Atmos. Environ*., 2011, **45**, 1725.
30 S. Deng, M. Bai and X. Bai, *Journal of Dalian Maritime University*, 2004, **3**, 62.
31 C. von Sonntag, *Adv. Quantum Chem*., 2007, **52**, 5.
32 G. Pramod, K. P. Prasanthkumar and H. Mohan, *J. Phys. Chem. A.*, 2006, **110**, 11517.

Table 1 The reaction barriers ($\Delta G^{\neq}$) and reaction Gibbs free energies (ΔG) at 298 K, all in kcal mol^{-1}, for the •OH + uridine in the gas, water and benzene phases, and •OH + uracil reaction in gas phase.

			•OH +uridine					•OH +uracil	
path	$\Delta G^{\neq}_{gas}$	ΔG_{gas}	$\Delta G^{\neq}_{water}$	ΔG_{water}	$\Delta G^{\neq}_{benzene}$	$\Delta G_{benzene}$	path	$\Delta G^{\neq}_{gas}$	ΔG_{gas}
cis-U5OH	1.87	-10.11	4.00 (3.69*)	-6.92 (-6.30*)	1.50	-9.54	U5OH	4.55	-10.30
trans-U5OH	3.98	-8.95	4.61 (4.10*)	-6.57 (-6.78*)	2.97	-9.52			
cis-U6OH	5.74	-12.74	7.31	-8.28	4.41	-10.27	U6OH	4.63	-12.97
trans-U6OH	5.58	-10.28	6.63	-8.49	4.85	-10.87			
UN3H8	9.11	-0.82	11.56	-4.17	8.60	-4.98	UN3H8	10.67	3.55
UC5H10	10.75	0.75	12.76	-0.49	10.06	-1.49	UC5H10	11.34	1.38
UC6H11	12.48	-4.75	14.76	-6.84	11.85	-5.70	UC6H11	9.51	-5.35

* The reaction barriers and reaction Gibbs free energies of *cis*-U5*wa*OH and *trans*-U5*wa*OH paths

Table 2 The rate constants (dm^{-3} mol^{-1} s^{-1}) for •OH + uridine reaction and branching ratios at 298 K and 310 K using the CVT/SCT method

	Gas		Water		Benzene	
	298 K	310 K	298 K	310 K	298 K	310 K
$k_{overall}$	2.39×10^{10}	1.78×10^{10}	2.74×10^{9}	2.24×10^{9}	8.01×10^{10}	5.57×10^{10}
$\Gamma_{cis\text{-U5OH}}$	0.716	0.665	0.622	0.590	0.701	0.653
$\Gamma_{trans\text{-U5OH}}$	0.239	0.279	0.356	0.383	0.268	0.308
$\Gamma_{cis\text{-U6OH}}$	0.022	0.028	0.008	0.010	0.015	0.019
$\Gamma_{trans\text{-U6OH}}$	0.022	0.028	0.013	0.016	0.015	0.019
Γ_{UN3H8}	0.001	0.001	0.000	0.000	0.001	0.002
Γ_{UC5H10}	0.000	0.000	0.000	0.000	0.000	0.000
Γ_{UC6H11}	0.000	0.000	0.000	0.000	0.000	0.000

Figure Captions

Fig.1 Schematic representation of the studied paths of reaction.

Fig.2 (a)B3LYP/6-311+G(d,p) optimized geometry of uridine with selected bond lengths (Å) and (b) the HOMO of uridine.

Fig.3 Optimized geometries of the •OH+uridine transition states and adducts along with imaginary frequencies for TSs.

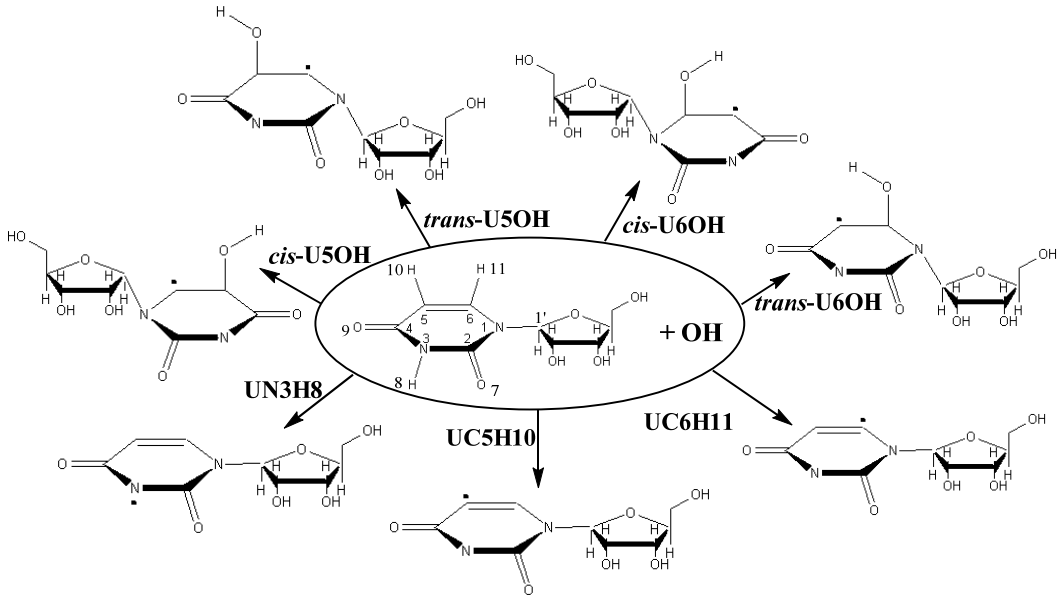

Fig. 1

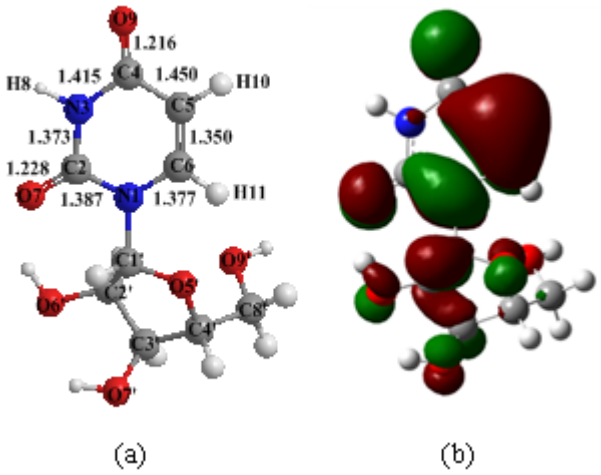

Fig. 2

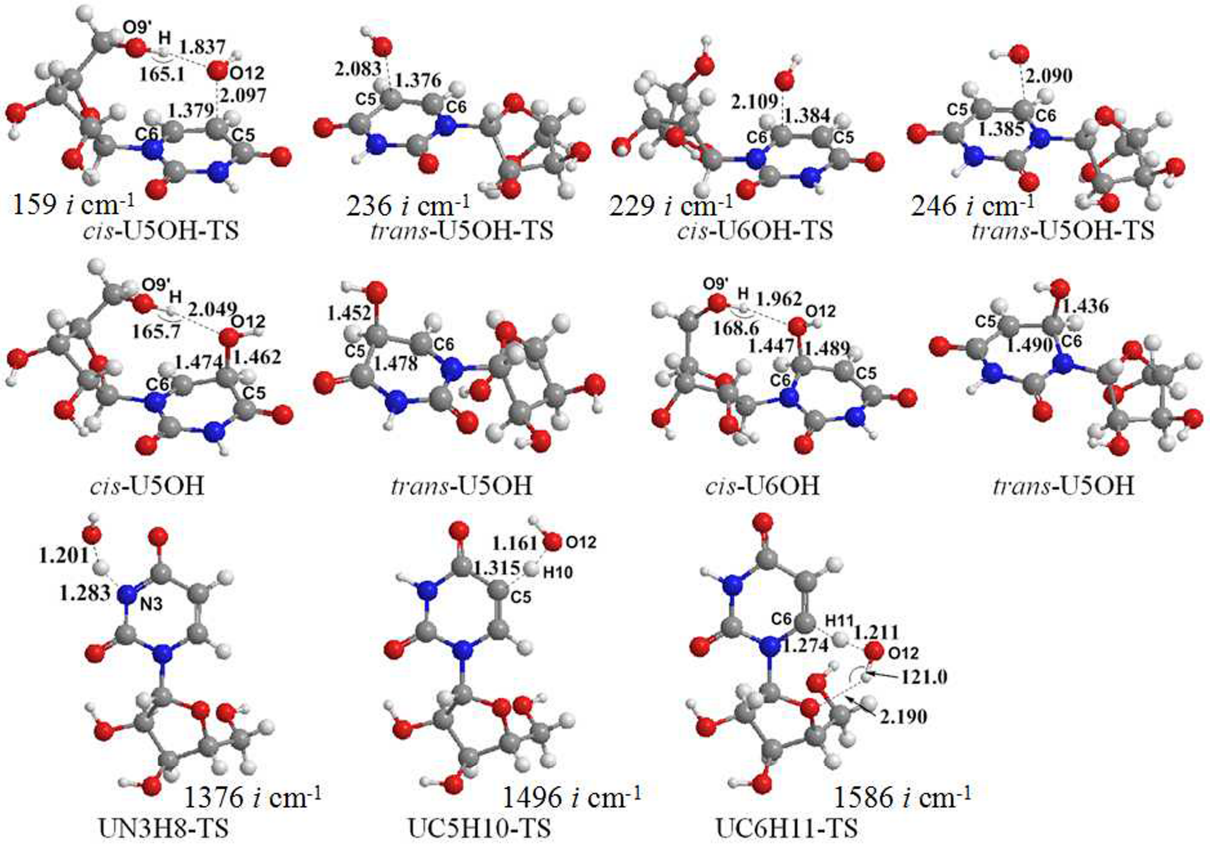

Fig. 3